

**Extended unitarity and absence of skin effect in periodically driven systems**Aditi Chakrabarty<sup>✉\*</sup> and Sanjoy Datta<sup>✉†</sup>*Department of Physics and Astronomy, National Institute of Technology, Rourkela, Odisha-769008, India*

(Received 24 April 2024; revised 19 June 2024; accepted 16 July 2024; published 15 August 2024)

One of the most striking features of non-Hermitian quasiperiodic systems with arbitrarily small asymmetry in the hopping amplitudes and open boundaries is the accumulation of all the bulk eigenstates at one of the edges of the system, termed in the literature as the *skin effect* (SE), below a critical strength of the potential. In this work, we uncover that a time-periodic drive in such systems can eliminate the SE up to a finite strength of this asymmetry. Remarkably, the critical value for the onset of SE is independent of the driving frequency and approaches to the static behavior in the thermodynamic limit. We find that the absence of SE is intricately linked to the emergence of *extended unitarity* in the delocalized phase, providing dynamical stability to the system. Interestingly, under periodic boundary condition, our non-Hermitian system can be mapped to a Hermitian analog in the large driving frequency limit that leads to the extended unitarity, irrespective of the hopping asymmetry and the strength of the quasiperiodic potential, in stark contrast to the static limit. Additionally, we numerically verify that this behavior persists at all frequencies of the drive. Based on our findings, we propose a possible experimental realization of our driven system, which could be used as a switch to control the light-funneling mechanism.

DOI: [10.1103/PhysRevB.110.064314](https://doi.org/10.1103/PhysRevB.110.064314)**I. INTRODUCTION**

In recent years, non-Hermitian Hamiltonians have garnered widespread attention due to their ability to accurately mimic experimental procedures involving interactions with the environment. They also offer possibilities for exotic phases of quantum matter that are typically absent in their Hermitian counterparts. Unlike Hermitian systems, the reality of eigenenergies and stable unitary dynamics is guaranteed only in specific classes of non-Hermitian Hamiltonians that possess either  $\mathcal{PT}$  symmetry [1,2] or pseudo-Hermiticity [3,4].

Among the non-Hermitian systems, the paradigmatic Hatano-Nelson (HN) Hamiltonian with asymmetric hopping amplitude [5,6] stands out as another class of non-Hermitian systems of particular interest. This interest stems from a unique phenomenon known as the *skin effect* (SE), which refers to the exponential localization of all bulk eigenstates at the edges of a lattice with an open boundary [7–12]. Interestingly, the spectral behavior in these systems is drastically sensitive to the choice of boundary conditions [13]. Moreover, recent studies have illustrated the existence of SE accompanying a delocalization-localization (DL) phase transition in such non-Hermitian quasicrystals [14].

In parallel, the exploration of a diversified range of periodically driven systems has been triggered due to the presence of rich and intriguing features typically absent in their temporally static counterparts [15–19]. The underlying quantum mechanics and the general understanding of such systems influenced by some external time-periodic drive (generally

known as Floquet systems) have gained interest in recent years due to their applications in ultrafast spintronics [20,21], quantum optics [22], ultracold atomic systems [23,24], and trapped ions [25]. On the other hand, the interplay between periodic driving and non-Hermiticity has led to several novel findings in recent years [26–33]. It has been demonstrated that a time-periodic drive can induce SE in systems with an on-site loss [34]. Additionally, Floquet engineering has been utilized to control the direction of edge modes [35]. Furthermore, it has been pointed out that a time-periodic drive can stabilize the dynamics of a two-level non-Hermitian Rabi model [36], where the Floquet quasienergies turn out to be real, leading to *extended unitarity* (EU) at the end of each complete driving period.

In this work, we unveil that a time-periodic drive can lead to the EU condition in HN quasicrystals, with a concurrent disappearance of the SE up to a finite strength of the nonreciprocity in the hopping amplitudes. In the limit of high frequency in the drive, we illustrate analytically that such a time-periodic modulation reduces the non-Hermitian system to a Hermitian equivalent counterpart under the periodic boundary condition (PBC), giving rise to completely real Floquet quasienergies irrespective of the strength of the potential and the asymmetry in the hopping amplitude, at each stroboscopic time period. This is in stark contrast to static HN quasicrystals, where the energy spectrum undergoes a complex to real transition at a critical value of the potential, although both of these systems manifest a DL transition. However, unlike the situation under PBC, the EU condition persists only up to a critical strength of the nonreciprocity in the delocalized regime under an open boundary condition (OBC). Interestingly, we demonstrate that the emergence of EU destroys the SE. Moreover, contrary to the static limit, where the

\*Contact author: [aditichakrabarty030@gmail.com](mailto:aditichakrabarty030@gmail.com)†Contact author: [dattas@nitrkl.ac.in](mailto:dattas@nitrkl.ac.in)

energies are real in the SE phase, we find that in time-periodic systems, it can exist when the Floquet quasienergy spectrum is complex. These counterintuitive results on the relationship between the SE and the eigenenergies completely alter our understanding of conventional HN systems.

In practice, from the perspective of experimentalists, it is noteworthy that the dynamics in such systems has found wide realizations in photonics and in quantum systems by enhancing the extent of optical sensing [37,38]. Additionally, the dynamics in a Hamiltonian with asymmetric hopping has recently been studied experimentally in photonic lattices to focus an incident light at a desired location, irrespective of the point of excitation, a phenomenon termed as light funneling [39]. In this work, we propose an experimental setup that can exploit our findings to tune the light-funneling effect.

The rest of the work is organized as follows. We begin by introducing our non-Hermitian time-periodic Hamiltonian in Sec. II A. Such driven systems are described within the framework of Floquet formalism, as elaborated in Sec. II B. The numerical technique used to locate the DL transition is elucidated in Sec. III. In the subsequent part of our work, we have demonstrated the important findings on the DL transition analytically in the regime of a large driving frequency in Sec. IV A, followed by the estimation of the phase boundaries in our driven system in Sec. IV B. In the next section (Sec. IV C), the absence of SE and its connection to the EU is established numerically, and the system-size behavior of SE is discussed. An experimental realization of the time-periodic Hamiltonian is proposed in Sec. V. Finally, the important highlights in this work are outlined in Sec. VI.

## II. THE PERIODICALLY DRIVEN SYSTEM

### A. The non-Hermitian quasiperiodic system under a drive

We consider a time-dependent version of the single-particle quasiperiodic non-Hermitian Hamiltonian [14,40] defined as

$$\begin{aligned} \mathcal{H}(t) = & \sum_{n=1}^{N-1} (J e^{h \cos(\omega t)} c_{n+1}^\dagger c_n + J e^{-h \cos(\omega t)} c_n^\dagger c_{n+1}) \\ & + \sum_{n=1}^N V \cos(2\pi \alpha n) c_n^\dagger c_n, \end{aligned} \quad (1)$$

where  $c_n^\dagger$  and  $c_n$  denote the fermionic creation and annihilation operators,  $N$  represents the number of sites in the lattice, and  $n$  is the site index. The lattice size  $L = Na$ , where  $a$  is the lattice period of translation (considered to be 1 in arb. units). In the prototypical static HN Hamiltonian, the asymmetric hopping of the fermions towards the left and the right is incorporated in the tight-binding notation using an imaginary magnetic vector potential by the terms  $e^{-h}$  and  $e^h$ , respectively. In this work, we consider continuous temporally cosine modulated nonreciprocal hopping amplitudes, as indicated in the first term of the above Hamiltonian. The second term characterizes the on-site quasiperiodic potential of the Aubry-André-Harper (AAH) type [41,42], where  $\alpha$  defines the incommensurability, set as  $(\sqrt{5} - 1)/2$  throughout this work.

### B. The Floquet theory

From the Hamiltonian described in Eq. (1), it is evident that after a stroboscopic period  $T$ ,  $\mathcal{H}(t) = \mathcal{H}(t + T)$ . For such time-periodic Hamiltonians, the Floquet theory has been instrumental in determining the states after a time  $T$ . According to the Floquet theory, the Floquet propagator for one complete period and an initial time  $t_0 = 0$  is defined as

$$U(T, 0) = \mathcal{T} e^{-i/\hbar \int_0^T \mathcal{H}(t) dt} = e^{-i\mathcal{H}_F T/\hbar}, \quad (2)$$

where  $\mathcal{T}$  takes care of the time ordering of the Hamiltonians at different instants of time. In the above equation,  $\mathcal{H}_F$  is the Floquet Hamiltonian, whose eigenstates can be obtained by the exact diagonalization of  $U(T, 0)$ . The reduced Planck's constant ( $\hbar$ ) is considered to be of unit magnitude throughout this work. In general,  $U(T, 0)$  is nonunitary when the elemental Hamiltonian is non-Hermitian and can be constructed using the biorthogonal formalism [43].

The eigenvectors and eigenvalues of  $U(T, 0)$  on exact diagonalization yield the eigenspectrum of  $\mathcal{H}_F$  given as

$$U(T, 0) = \sum_n E_n |\psi_{nR}\rangle \langle \psi_{nL}| \quad \text{and} \quad E_n = e^{-i\epsilon_n^F T}, \quad (3)$$

where  $E_n$ ,  $|\psi_{nR}\rangle$ , and  $|\psi_{nL}\rangle$  are the eigenenergies and the right and left eigenvectors, respectively. The Floquet quasienergies  $\epsilon_n^F$  satisfy the relation  $\mathcal{H}_F \psi_n = \epsilon_n^F \psi_n$  (defined modulo  $\hbar\omega$ ). The solutions to the time-dependent Hamiltonian to ascertain the physical properties can mostly be attained numerically using the Floquet eigenstates and quasienergies as described above [44].

## III. CHARACTERIZATION OF THE DELOCALIZATION-LOCALIZATION (DL) PHASE TRANSITION

To identify the delocalized and localized phases in the system, the concept of inverse participation ratio (IPR) [45,46] is widely used in the literature. The IPR has been extended in non-Hermitian systems, where a new measure of bidirectional-IPR (BIPR) for an eigenstate labeled “ $j$ ” has been introduced recently [47] and is defined as

$$\text{BIPR}_j = \frac{\sum_{n=1}^N |\psi_{nL}^j \psi_{nR}^j|^2}{\left(\sum_{n=1}^N |\psi_{nL}^j \psi_{nR}^j|\right)^2}, \quad (4)$$

where the sum of the weights of the wave vectors is over all the lattice sites indicated by  $n$ .  $\langle \text{BIPR} \rangle$  signifies the average of BIPR over all the eigenstates. The  $\langle \text{BIPR} \rangle$  is  $O(L^{-1})$  when the states are completely delocalized, and  $O(1)$  in the localized regime. For all the subsequent details and the findings on our periodically driven system, we have considered  $J = 1$  (in arb. units),  $L = 144$ , and the Trotter time step as  $\Delta t = 0.001$ , unless specifically stated.

## IV. RESULTS AND DISCUSSIONS

The aim of this work is achieved in two steps. We first explore the behavior of the DL transition of the time-dependent HN system under PBC in the parameter space of  $h$  and  $V$  for different driving frequencies. In the subsequent analysis, we

assess the sensitivity of the energy spectrum to the boundary conditions along with the investigation of the existence of SE.

### A. Analytical understanding of the DL transition in the high-frequency regime

In the following, we demonstrate that the critical point of the DL transition under the PBC can be obtained analytically in the regime of a large frequency of the drive. The analytical expression of the phase boundary is derived by retrieving an effective Floquet Hamiltonian upon time averaging the original Hamiltonian, as discussed in earlier works [48–51]. Such an expression of the effective Floquet Hamiltonian was originally derived starting from the spatially periodic Schrödinger equation in Hermitian systems, which obey the well-known bulk-boundary correspondence [48]. However, the non-Hermitian system as considered in this work alters the nature of the bulk states depending on the choice of the boundary conditions, violating such a bulk-boundary correspondence. Naturally, the analytical results obtained under the PBC cannot predict the nature of the states and its dynamics under the OBC, except the critical point for the localization transition. The effective Hamiltonian, which can only be obtained when the frequency of the drive is large enough, is written as follows:

$$\mathcal{H}_F = \frac{1}{T} \int_0^T \mathcal{H}(t) dt. \quad (5)$$

To evaluate  $\mathcal{H}_F$  as given in Eq. (5), we first consider the hopping towards the right, which is given by

$$\frac{1}{T} \int_0^T \sum_n (J e^{h \cos(\omega t)} c_{n+1}^\dagger c_n) dt. \quad (6)$$

In the above equation,  $\int_0^T e^{h \cos(\omega t)} dt$  can be identified as the generating function of the modified Bessel equation, i.e.,  $\int e^{\frac{z}{2}(x+\frac{1}{x})} dx$  with  $z = h$  and  $x = \exp(i\omega t)$ . Integration over the entire time period yields the effective Floquet Hamiltonian for this part, and is given as

$$\sum_n [J \mathcal{I}_0(h)] c_{n+1}^\dagger c_n, \quad (7)$$

where  $\mathcal{I}_0$  is the zeroth-order modified Bessel function. It is interesting to note that the above expression is independent of  $\omega$ . Similarly, for the hopping in the opposite direction (towards the left), the other part of the effective Hamiltonian can be written as

$$\sum_n [J \mathcal{I}_0(-h)] c_n^\dagger c_{n+1}. \quad (8)$$

It is easy to see that  $\mathcal{I}_0(h) = \mathcal{I}_0(-h)$ . The effective Floquet Hamiltonian can then be explicitly written as

$$\begin{aligned} \mathcal{H}_F = & \sum_n [J \mathcal{I}_0(h)] (c_{n+1}^\dagger c_n + c_n^\dagger c_{n+1}) \\ & + \sum_n V \cos(2\pi \alpha n) c_n^\dagger c_n. \end{aligned} \quad (9)$$

Remarkably, from Eq. (9), it becomes quite evident that the effective Floquet Hamiltonian for the HN systems with a drive in the magnetic vector potential reduces to a Hermitian

AAH Hamiltonian with a rescaled hopping amplitude given as  $J \mathcal{I}_0(h)$  in the regime of high frequency. Thus, we expect the DL transition to occur at a critical value of the quasiperiodic potential determined by the self-duality of the AAH Hamiltonian in the Hermitian limit, expressed as

$$V_c = 2J', \quad \text{where } J' = J \mathcal{I}_0(h). \quad (10)$$

### B. Phase diagram at different driving frequencies

Figures 1(a)–1(d) illustrate the phase diagram of the time-periodic version of the HN Hamiltonian as discussed in Eq. (1) under the PBC. In sharp contrast to the static system, interestingly, we observe from Figs. 1(a)–1(d) that the DL transition (indicated by a transition from blue to a different color) does not follow the critical value of the undriven system (indicated by the solid red line) determined from the condition  $V_c = \max[Je^h, Je^{-h}]$ , as demonstrated in Ref. [40]. From the phase diagrams, it is evident that the transition from delocalized to localized states strongly depends on the driving frequency.

In Figs. 1(a)–1(d), we have indicated the analytically obtained phase boundary in Eq. (10) by a black dotted line. It is clear that as we approach to a higher value of the driving frequency ( $\omega = 4\pi$ ), the numerically determined critical value for the DL transition agrees excellently with the analytical result in the entire parameter space. However, for lower driving frequencies, the numerical critical points follow the analytical expression only up to a certain strength of the asymmetry. In addition, the effect of the periodic drive in such systems is to shift the DL transition to a lower value of  $V_c$ , as compared to its static counterpart [demonstrated by the red line in Figs. 1(a)–1(d)]. Moreover, our analytical result suggests that the Floquet quasienergies in the entire parameter space of  $h$  and  $V$  should be real for high driving frequencies under PBC, due to the exact mapping of the original non-Hermitian system to the Hermitian AAH Hamiltonian. We have numerically verified this assertion. Surprisingly, however, the reality of the quasienergies persists for all frequencies of the drive. This is in complete contrast to the static HN Hamiltonian under the PBC, where the DL transition is concurrent with a spectral transition from complex to real. In our case, the existence of the real quasienergies irrespective of the strength of the potential (refer to Fig. 6 in Appendix A more details) and non-Hermiticity, which is the hallmark for EU, suggests that our system becomes dynamically stable after a stroboscopic driving period.

### C. Skin effect under the drive

In such non-Hermitian systems with asymmetric hopping, a change in the boundary condition from PBC to OBC drastically alters the behavior of electronic states and eigenenergies, especially in the delocalized phase. In the static HN counterparts, it has been well demonstrated that under the OBC, in the delocalized regime, the eigenenergies lie on the real axis [11], along with the appearance of SE. Naturally, one of the most important question that arises is whether such a correspondence between the quasienergies and SE exists under the time-periodic drive. We address this question in the subsequent discussion.

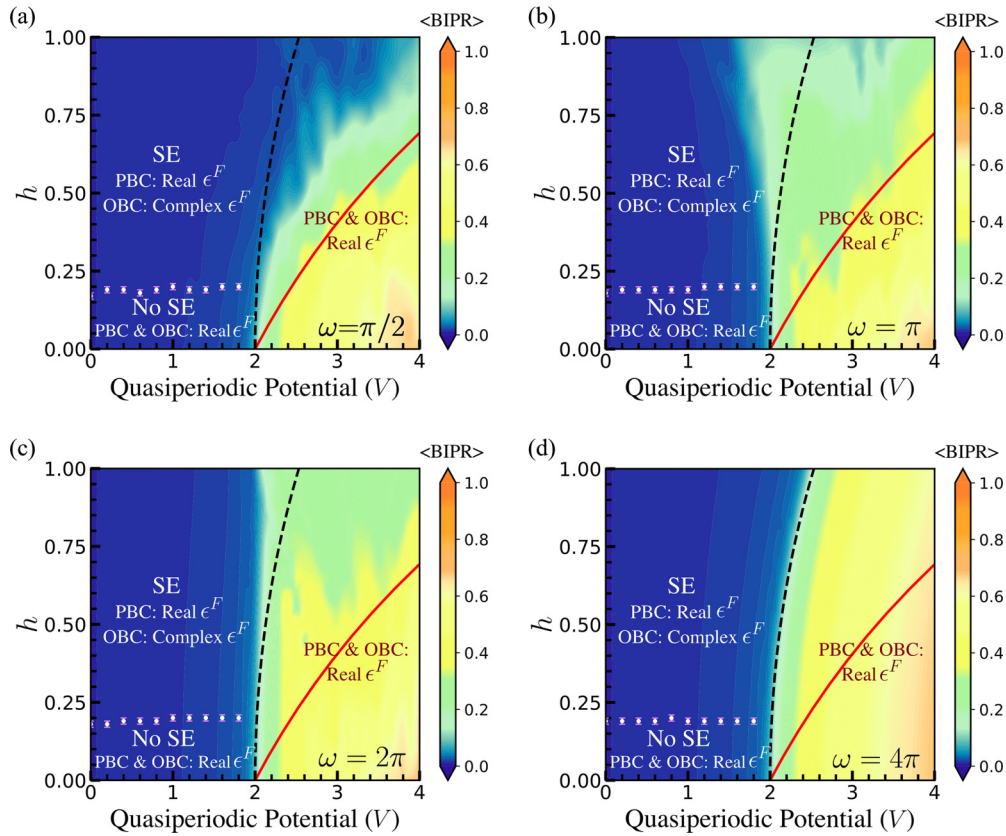


FIG. 1. Projected  $\langle \text{BIPR} \rangle$  as a function of  $h$  and  $V$  for the driven HN system at different driving frequencies: (a)  $\omega = \pi/2$ , (b)  $\omega = \pi$ , (c)  $\omega = 2\pi$ , and (d)  $\omega = 4\pi$ . The blue region in all the phase diagrams indicates the delocalized phase. The red solid line depicts the critical point for the DL transition in the static HN Hamiltonian. The black dotted lines manifest the critical value under the drive as obtained analytically from the expression in Eq. (10). The DL transition is demonstrated for a lattice with 144 sites and under the PBC. The white data markers superposed in all the phase diagrams separate the regions with and without the SE, obtained under OBC. The spectral behavior in the different regimes under both PBC and OBC is also indicated.

In analogy with the static system, one can naively anticipate that the SE would persist in the entire delocalized regime [represented in blue in Figs. 1(a)–1(d)] retaining the reality of the Floquet quasienergies. However, we demonstrate that this expectation is in complete contradiction when the system is driven. From Figs. 2(a) and 2(c), it is evident that for weak asymmetry in the hopping, the periodic drive leads to real Floquet quasienergies under both the periodic and open boundary conditions. However, remarkably, we find that under the OBC, the time-periodic drive demolishes the SE regardless of the driving frequency [Figs. 2(b) and 2(d)], contrary to the undriven systems where the SE exists for an arbitrarily weak strength of the imaginary magnetic vector potential.

To further understand the dependence of the SE on  $h$ , we consider a slightly greater amplitude of the asymmetry in the Hamiltonian. In this case, the quasienergy spectrum under the PBC still exhibits real eigenvalues, similar to a Hermitian system, as demonstrated in Figs. 3(a) and 3(c), manifesting EU as indicated previously. This is in accordance with the finding in Eq. (9). However, with an increase in the value in  $h$ , the spectrum under OBC lies on the complex plane and does not satisfy the EU condition. Surprisingly, when the spectrum becomes complex under OBC, the system exhibits SE irrespective of the driving frequency, as illustrated in Figs. 3(b) and 3(d). This is in stark contrast to the static systems. From

these findings, it is clear that there exists a critical value  $h_c$  at which the SE appears.

Furthermore, from the above findings, it is easy to see that the states dynamically accumulate at the boundaries after a stroboscopic time evolution when the extended unitarity is broken. This can be understood from the Floquet propagator ( $U = e^{-i\mathcal{H}_F T}$ ). When the Floquet quasienergies of  $\mathcal{H}_F$  are real, the propagator accumulates real phase factors, which do not alter the mechanism of localization in the regime that we label as EU. However, when  $\mathcal{H}_F$  gives rise to complex quasienergies (in the broken EU regime), there is a growth or decay of the wave functions governed by the Floquet propagator. This is similar to the basic phenomenon required for SE, i.e., an amplification in one direction and a decay towards the other direction. This exponential growth/decay results in the localization of the modes towards the edge of the lattice, i.e., the SE, when the EU condition is broken.

We have numerically determined  $h_c$  in the entire parameter space of  $h$  and  $V$ . Our findings are summarized in Figs. 1(a)–1(d) for different frequencies of the drive. It is remarkable that  $h_c$  is independent of the driving frequency and the quasiperiodic potential. The numerical value of  $h_c$  is estimated to be  $h \simeq 0.20$  with an error of  $\pm 0.01$ . The preceding discussions clearly indicate that the emergence of EU and disappearance of SE are closely linked in such driven systems. The

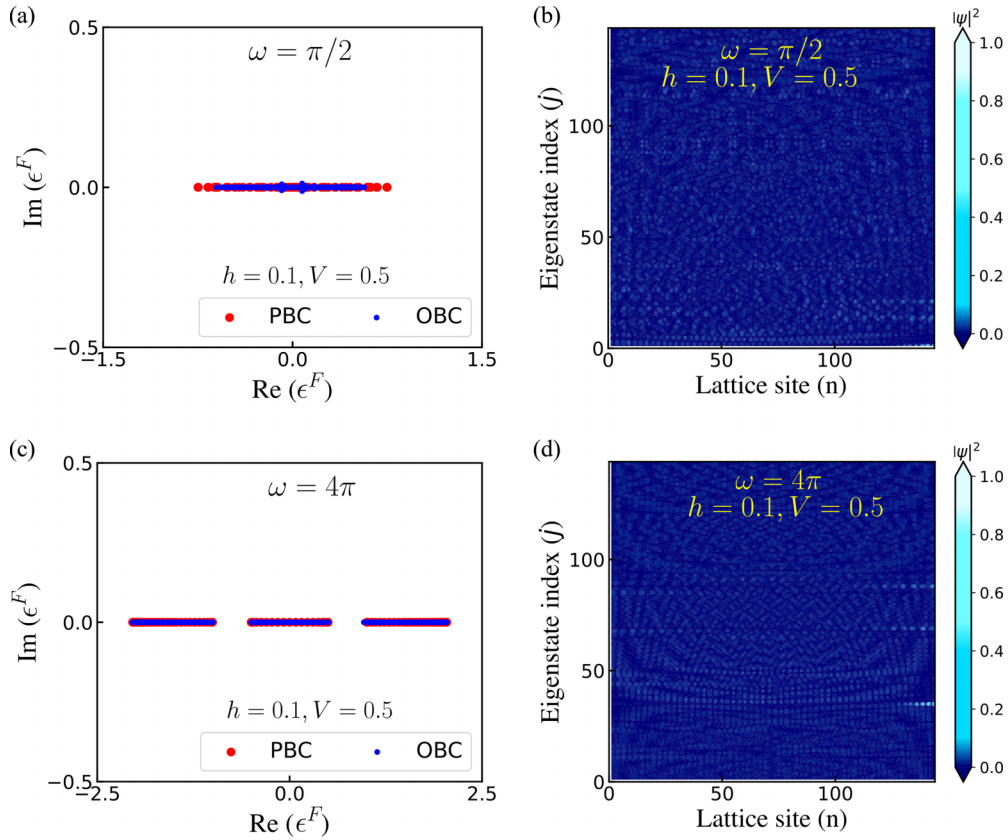


FIG. 2. The Floquet quasienergy spectrum under the PBC (red) and OBC (blue) for the driven system at a low value of the imaginary vector potential, i.e.,  $h = 0.1$  and  $V = 0.5$  at (a)  $\omega = \pi/2$  and (c)  $\omega = 4\pi$ . (b),(d) Lattice-site resolved  $|\psi|^2$  for all the eigenstates corresponding to the two parameters in (a) and (c), respectively, indicating the absence of SE under the OBC.  $L = 144$  in all the cases.

determination of  $h_c$  for the different driving frequencies has been elucidated in Fig. 7 in Appendix B.

It is important to note that the critical strength of the asymmetricity for the onset of SE in such driven systems strongly depends on the size of the lattice. In order to get a comprehensive idea of this system-size dependence, in Fig. 4 we present  $h_c$  as a function of  $1/L$  for different driving frequencies. It is evident that  $h_c$  scales inversely with the system size. In addition,  $h_c$  becomes independent of the driving frequency when the size of the lattice is large enough. Furthermore, it can be easily observed that  $h_c$  approaches to the static limit of HN Hamiltonian for  $L \rightarrow \infty$ .

The existence of  $h_c$  for the SE and EU condition along with its system-size dependence can be understood from the behavior of the instantaneous eigenstates of the original time-dependent Hamiltonian given in Eq. (1). We find that at  $t = 0$ , the Hamiltonian possesses a greater hopping amplitude towards the right. For any given driving frequency and a fixed  $L$ , it is easy to see that within a stroboscopic period, there are two sign changes in the hopping amplitude terms, i.e.,  $Je^{h\cos(\omega t)}$  and  $Je^{-h\cos(\omega t)}$ . This suggests that after a complete stroboscopic period, the states will be accumulated towards the right edge, which agrees with our observation reported for  $h > h_c$ . However, for  $h < h_c$ , a detailed observation reveals that the difference between the two asymmetric hopping amplitudes remains close to zero for larger instances of time due to the small value of  $h$ . Moreover, the amplitude of

the skin modes is found to be pretty weak. Therefore, the time averaging washes out the effect of the asymmetry in the hopping amplitudes. On the other hand, for large  $h$ , the difference in the hopping asymmetry is large enough for most instances of time, thereby giving rise to larger amplitude of the skin states and an overall right unidirectionality at the end of the complete driving period. In addition, for a fixed value of  $h$ , at any instant of time, we find that the wave-function amplitude decreases as we move away from the edge (which is an anticipated behavior owing to the SE). This is, in general, true for all system sizes. However, we found that as the system size becomes smaller, say  $L = 89$ , the amplitudes at far away sites do not completely vanish. Therefore, on time averaging, the SE effectively vanishes in smaller systems because of a comparable magnitude at all lattice sites. On the other hand, at the same value of  $h$ , with an increase in the size of the lattice, say  $L = 233$ , the wave-function probabilities at sites distant to the edges fall off to zero. Since in an entire stroboscopic period the system has a greater tendency towards the right for most of the time instances, the time averaging results in vanishingly small amplitudes away from the right edge, eventually giving rise to a SE at the right. This results in a decrease in the value of  $h_c$  with an increase in  $L$ .

Our findings in this work reveal that although the SE appears at even an arbitrarily small strength of the asymmetry in static HN Hamiltonian, a time-periodic drive can eliminate the SE up to some critical strength of asymmetricity, i.e.,  $h_c$ ,

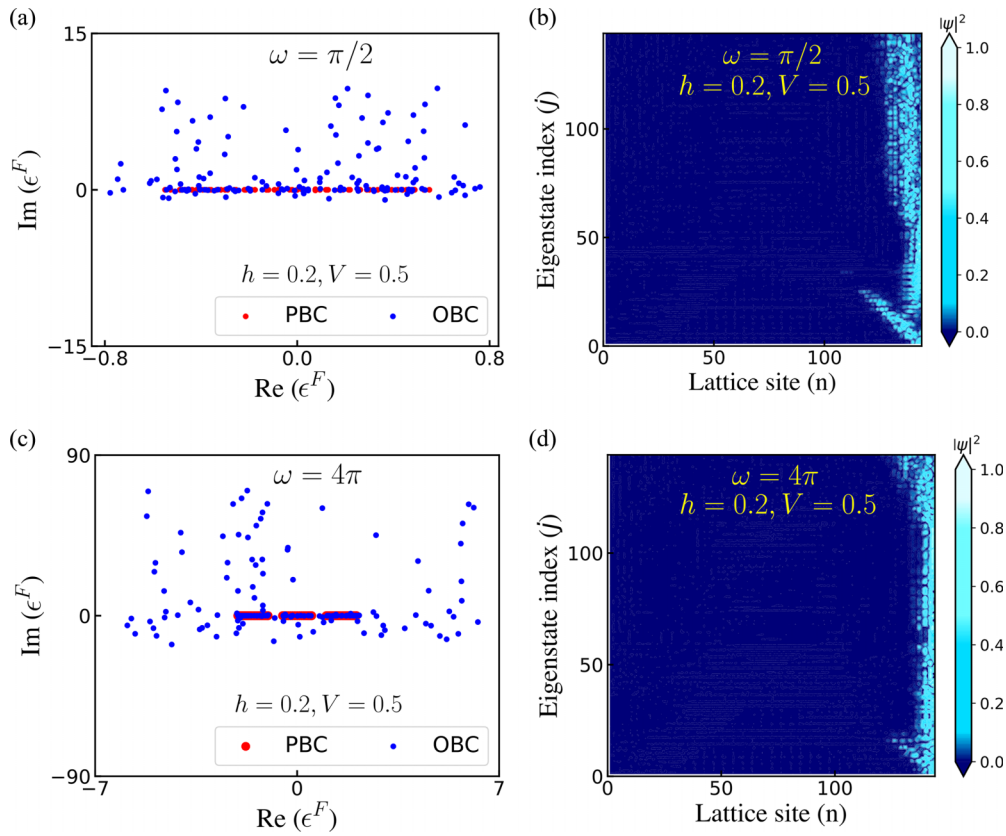


FIG. 3. The Floquet quasienergy spectrum under the PBC (red) and OBC (blue) for the driven system at  $h = 0.2$  and  $V = 0.5$  at (a)  $\omega = \pi/2$  and (c)  $\omega = 4\pi$ . (b),(d) Lattice-site resolved  $|\psi|^2$  for different eigenstates for the two parameters corresponding to (a) and (c), demonstrating the presence of SE under the OBC. The lattice consists of 144 sites in all the cases.

at least up to a certain finite size of the driven lattice. Our result paves the way to control the SE either by controlling the strength of the asymmetry in the hopping or the size of the lattice. An interesting experimental implementation of regulating the SE using these two mechanisms is presented in Sec. V.

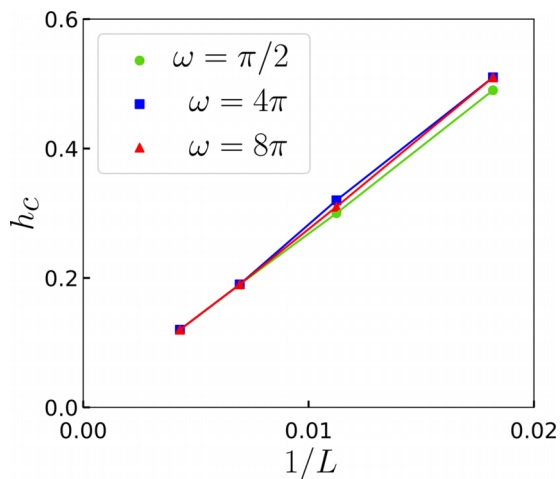


FIG. 4. System-size behavior of  $h_c$  for the onset of SE as a function of inverse lattice size in different regimes of the Floquet drive, i.e., at  $\omega = \pi/2$  (green),  $\omega = 4\pi$  (blue), and  $\omega = 8\pi$  (red). The data are obtained for  $L = 55, 89, 144,$  and  $233$  under the OBC.

## V. EXPERIMENTAL IMPLEMENTATION: SWITCH FOR LIGHT FUNNELING

In this discussion, we propose a possible experimental implementation of the system considered in this work from the point view of its application in controlling the light-funneling effect. Similar to the recent realizations of the nonreciprocal lattices in photonic systems as demonstrated in Refs. [39,52], we consider a setup with two optical fibers with anisotropic hopping in either direction, separated by an interface as illustrated in Fig. 5. The driven HN system can be replicated by changing the anisotropy in the hopping with the help of a frequency-dependent beam splitter [53], and selectively using the desired beam of light. Such an unidirectionality in the two fibers causes the incident light that is impinging on the lattice to be pushed towards the interface due to SE, resulting in a funneling effect of the output light. Since the value of  $h$  can be tuned with the anisotropic beam splitter and our results suggest the existence of  $h_c$  for the onset of SE, it is easy to understand that the SE can be turned on or off by controlling the beam splitter or by simply choosing an appropriate lattice size, effectively acting as a switch to tune the light-funneling effect.

## VI. CONCLUSIONS

In conclusions, this work demonstrates that a time-periodic drive can fundamentally alter the behavior of the paradigmatic quasiperiodic HN systems. By introducing a drive,

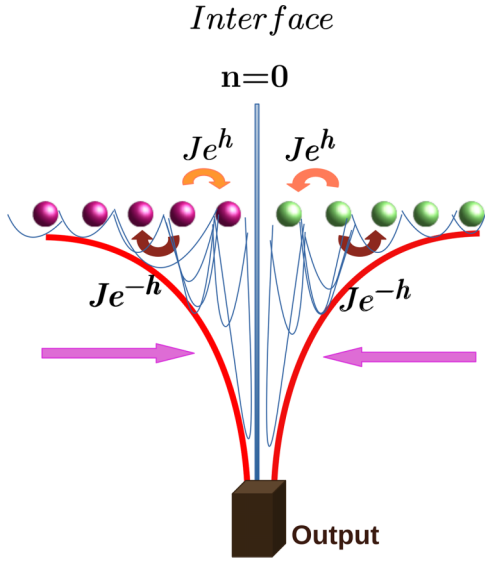


FIG. 5. Schematic of light funneling using two oppositely directed static HN chains. The interface is formed at  $n = 0$ . The chains on the left and right sides of the interface have greater unidirectionality towards the right and left directions, respectively. The output light traverses through the funnel-like structure where it is collected.

we unfold that under PBC, the Floquet Hamiltonian in the large-frequency limit becomes equivalent to a Hermitian AAH counterpart, giving rise to the extended unitarity and real Floquet quasienergies in the entire parameter space of the Hamiltonian, in stark contrast to the static limit. We find that the driven system undergoes a DL transition similar to the static case, albeit at a lower strength of the potential for a given asymmetry in the hopping, determined by the self-duality condition of the effective Hermitian AAH Hamiltonian. Under OBC, however, we find that the EU condition survives only up to a critical value of the asymmetry in the hopping,  $h_c$ , along with the disappearance of SE within that asymmetry. In complete contrast to the static limit, the SE appears above this critical value with complex Floquet quasienergies. Remarkably, for a given system size,  $h_c$  is found to be independent of the driving frequency and quasiperiodic potential. Furthermore, we find that  $h_c$  scales inversely with the system size

approaching to the static behavior in the thermodynamic limit. Our work deepens the understanding of the DL transition under the PBC, Floquet quasienergies, and its connection to the SE under the OBC in HN systems. Finally, we provide an experimental setup that can utilize the findings of this work to control the light-funneling mechanism.

## ACKNOWLEDGMENTS

A.C. acknowledges the financial support received from the Council of Scientific and Industrial Research (CSIR)-HRDG, India, via File No. 09/983(0047)/2020-EMR-I. The data computation in this work was carried out in the cluster procured from SERB (DST), India (Grant No. EMR/2015/001227) and using the High Performance Computing (HPC) facilities of the National Institute of Technology Rourkela.

## APPENDIX A: EXISTENCE OF EXTENDED UNITARITY IN THE LOCALIZED REGIME

In Figs. 1(a)–1(d) of the main text, we have illustrated the phase diagrams of the driven HN Hamiltonian considered in our work. It is well known that the delocalization-localization phase transition in the static Hatano-Nelson (HN) systems is accompanied by a complex to real transition in the energy spectrum under the periodic boundary condition (PBC). Under the open boundary condition (OBC), such systems exhibit the SE, as discussed in the main text. However, as we have demonstrated, in the driven systems and under the PBC, the Floquet quasienergies are always real in the delocalized regime, satisfying the extended unitarity (EU) condition, as shown in Figs. 2(a) and 2(c) and Figs. 3(a) and 3(c) in the main text for  $h = 0.1$  and  $h = 0.2$ , respectively. This is contrary to the behavior of static HN systems. Moreover, under the OBC, the Floquet quasienergy spectra changes from real [in the presence (absence) of EU (SE)] to complex [in the absence (presence) of EU (SE)]. To assess the behavior of the EU in the localized regime of the phase diagram, we have presented the quasienergy spectrum under both the PBC and OBC in Figs. 6(a) and 6(b). It is evident that for any frequency in the drive, the Floquet quasienergies satisfy the EU condition in the localized regime of the phase diagram under both of the

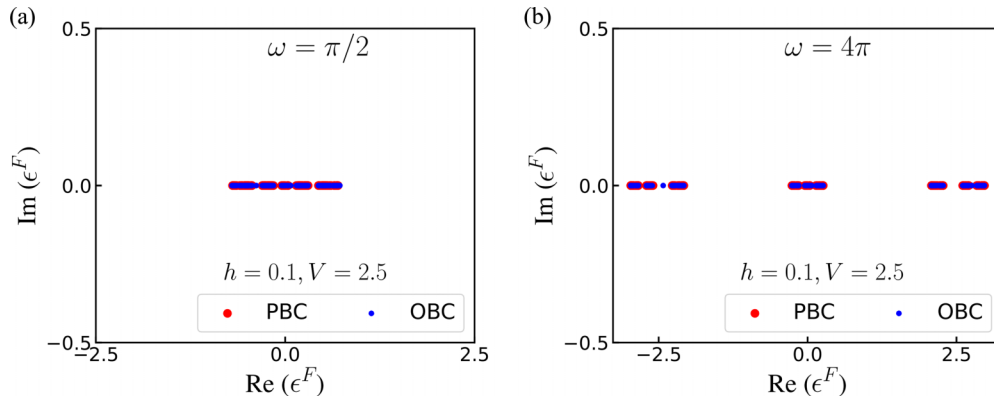


FIG. 6. The Floquet quasienergy spectrum in the complex plane under the PBC (in red) and OBC (in blue) at  $h = 0.1$  and  $V = 2.5$  (localized regime) at: (a)  $\omega = \pi/2$ , (b)  $\omega = 4\pi$ .  $L = 144$  as considered in the main text.

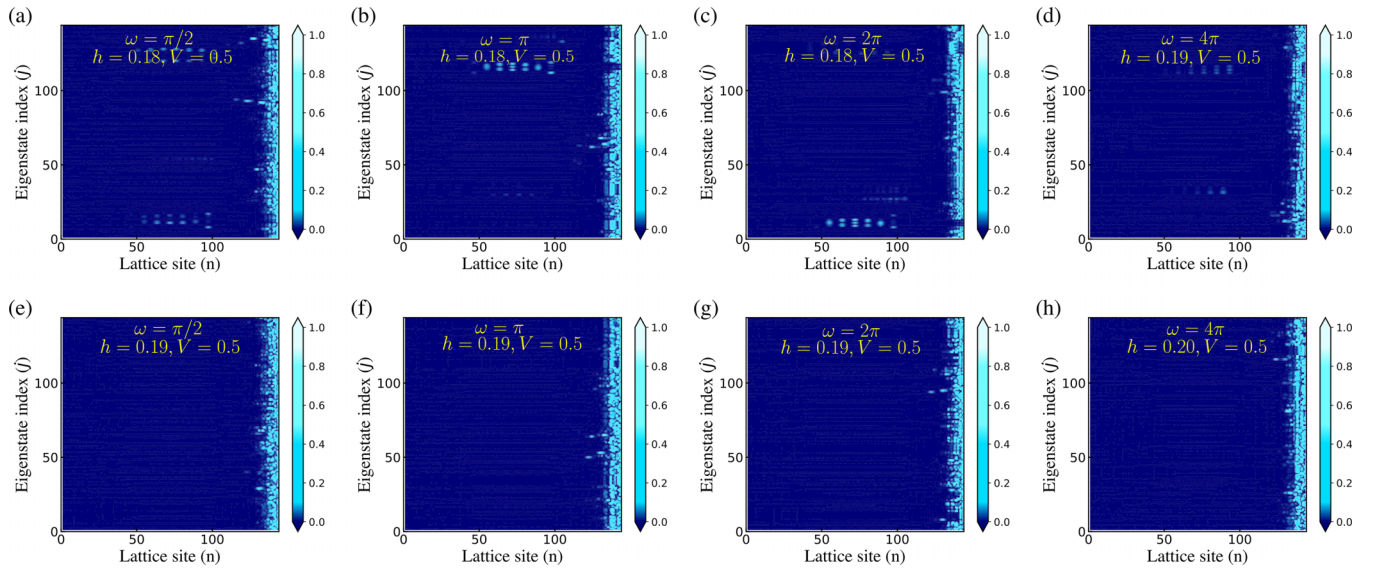


FIG. 7.  $|\psi|^2$  for all the eigenstates projected over the lattice sites at (a),(e)  $\omega = \pi/2$ , (b),(f)  $\omega = \pi$ , (c),(g)  $\omega = 2\pi$ , and (d),(h)  $\omega = 4\pi$ . The figures in the upper panel correspond to the value of  $h$  just before the onset of SE, whereas the ones in the lower panel correspond to the value of  $h$  at which the SE appears (determined within an error of  $\pm 0.01$ ). We have considered the OBC in a lattice with 144 sites.

boundary conditions. We have verified that this EU condition persists irrespective of the strength of the quasiperiodic potential and asymmetric hopping amplitude, as illustrated in Figs. 6(a) and 6(b).

## APPENDIX B: DEMONSTRATION OF SE IN THE DRIVEN HN SYSTEMS

To find out the critical value of  $h_c$  for the onset of SE, we resort to the conventional method of determining whether all of the eigenstates localize at one end of the lattice using the wave-function probabilities as demonstrated in

Figs. 7(a)–7(h). In an unidirectional system, all the eigenstates under the OBC pile up at one of the edges towards which there is a greater directionality of the fermionic hopping. Therefore, in our system, since the amplitude of hopping towards the right dominates over the left hopping amplitude, we say that our system possesses SE when all the states are localized towards the right end. It is clear from the upper panel of Figs. 7(a)–7(d), a few eigenstates are localized in the bulk of the system. Therefore, we do not consider them as skin modes. We have clearly illustrated the value of  $h_c$  at  $0.20 \pm 0.01$  for different driving frequencies in a lattice with 144 sites, as discussed in the main text.

- [1] C. M. Bender and S. Boettcher, Real spectra in non-Hermitian Hamiltonians having  $\mathcal{PT}$  symmetry, *Phys. Rev. Lett.* **80**, 5243 (1998).
- [2] C. M. Bender, M. V. Berry, and A. Mandilara, Generalized PT symmetry and real spectra, *J. Phys. A: Math. Gen.* **35**, L467 (2002).
- [3] A. Mostafazadeh, Pseudo-Hermiticity versus symmetry: The necessary condition for the reality of the spectrum of a non-Hermitian Hamiltonian, *J. Math. Phys.* **43**, 205 (2002).
- [4] K. Kawabata, K. Shiozaki, M. Ueda, and M. Sato, Symmetry and topology in non-Hermitian physics, *Phys. Rev. X* **9**, 041015 (2019).
- [5] N. Hatano and D. R. Nelson, Localization transitions in non-Hermitian quantum mechanics, *Phys. Rev. Lett.* **77**, 570 (1996).
- [6] N. Hatano and D. R. Nelson, Non-Hermitian delocalization and eigenfunctions, *Phys. Rev. B* **58**, 8384 (1998).
- [7] T. E. Lee, Anomalous edge state in a non-Hermitian lattice, *Phys. Rev. Lett.* **116**, 133903 (2016).
- [8] V. M. Martínez Alvarez, J. E. Barrios Vargas, and L. E. F. Foa Torres, Non-Hermitian robust edge states in one dimension: Anomalous localization and eigenspace condensation at exceptional points, *Phys. Rev. B* **97**, 121401(R) (2018).
- [9] C. H. Lee, L. Li, and J. Gong, Hybrid higher-order skin-topological modes in nonreciprocal systems, *Phys. Rev. Lett.* **123**, 016805 (2019).
- [10] D. S. Borgnia, A. J. Kruchkov, and R.-J. Slager, Non-Hermitian boundary modes and topology, *Phys. Rev. Lett.* **124**, 056802 (2020).
- [11] N. Okuma, K. Kawabata, K. Shiozaki, and M. Sato, Topological origin of non-Hermitian skin effects, *Phys. Rev. Lett.* **124**, 086801 (2020).
- [12] R. Shen, T. Chen, B. Yang, and C. Lee, Observation of the non-Hermitian skin effect and Fermi skin on a digital quantum computer, [arXiv:2311.10143](https://arxiv.org/abs/2311.10143).
- [13] Y. Xiong, Why does bulk boundary correspondence fail in some non-Hermitian topological models, *J. Phys. Commun.* **2**, 035043 (2018).
- [14] S. Longhi, Phase transitions in a non-Hermitian Aubry-André-Harper model, *Phys. Rev. B* **103**, 054203 (2021).
- [15] H. Lignier, C. Sias, D. Ciampini, Y. Singh, A. Zenesini, O. Morsch, and E. Arimondo, Dynamical control of matter-wave tunneling in periodic potentials, *Phys. Rev. Lett.* **99**, 220403 (2007).
- [16] V. V. Ivanov, A. Alberti, M. Schioppo, G. Ferrari, M. Artoni, M. L. Chiofalo, and G. M. Tino, Coherent delocalization of



- atomic wave packets in driven lattice potentials, *Phys. Rev. Lett.* **100**, 043602 (2008).
- [17] N. Poli, F.-Y. Wang, M. G. Tarallo, A. Alberti, M. Prevedelli, and G. M. Tino, Precision measurement of gravity with cold atoms in an optical lattice and comparison with a classical gravimeter, *Phys. Rev. Lett.* **106**, 038501 (2011).
- [18] Y.-A. Chen, S. Nascimbène, M. Aidelsburger, M. Atala, S. Trotzky, and I. Bloch, Controlling correlated tunneling and superexchange interactions with ac-driven optical lattices, *Phys. Rev. Lett.* **107**, 210405 (2011).
- [19] M. Bitter and V. Milner, Experimental observation of dynamical localization in laser-kicked molecular rotors, *Phys. Rev. Lett.* **117**, 144104 (2016).
- [20] T. Oka and S. Kitamura, Floquet engineering of quantum materials, *Annu. Rev. Condens. Matter Phys.* **10**, 387 (2019).
- [21] J. M. Losada, A. Brataas, and A. Qaiumzadeh, Ultrafast control of spin interactions in honeycomb antiferromagnetic insulators, *Phys. Rev. B* **100**, 060410(R) (2019).
- [22] C. J. Eckhardt, G. Passetti, M. Othman, C. Karrasch, F. Cavaliere, M. A. Sentef, and D. M. Kennes, Quantum Floquet engineering with an exactly solvable tight-binding chain in a cavity, *Commun. Phys.* **5**, 122 (2022).
- [23] F. Meinert, M. J. Mark, K. Lauber, A. J. Daley, and H.-C. Nägerl, Floquet engineering of correlated tunneling in the Bose-Hubbard model with ultracold atoms, *Phys. Rev. Lett.* **116**, 205301 (2016).
- [24] K. Sandholzer, A.-S. Walter, J. Minguzzi, Z. Zhu, K. Viebahn, and T. Esslinger, Floquet engineering of individual band gaps in an optical lattice using a two-tone drive, *Phys. Rev. Res.* **4**, 013056 (2022).
- [25] R. He, M.-Z. Ai, J.-M. Cui, Y.-F. Huang, Y.-J. Han, C.-F. Li, G.-C. Guo, G. Sierra, and C. E. Creffield, Riemann zeros from Floquet engineering a trapped-ion qubit, *npj Quantum Inf.* **7**, 109 (2021).
- [26] G. Della Valle and S. Longhi, Spectral and transport properties of time-periodic  $\mathcal{PT}$ -symmetric tight-binding lattices, *Phys. Rev. A* **87**, 022119 (2013).
- [27] C.-H. Liu, H. Hu, and S. Chen, Symmetry and topological classification of Floquet non-Hermitian systems, *Phys. Rev. B* **105**, 214305 (2022).
- [28] L. Zhou, Floquet engineering of topological localization transitions and mobility edges in one-dimensional non-Hermitian quasicrystals, *Phys. Rev. Res.* **3**, 033184 (2021).
- [29] Y. Huang, Z. Q. Yin, and W. L. Yang, Realizing a topological transition in a non-Hermitian quantum walk with circuit QED, *Phys. Rev. A* **94**, 022302 (2016).
- [30] T. T. Koutserimpas and R. Fleury, Nonreciprocal gain in non-Hermitian time-Floquet systems, *Phys. Rev. Lett.* **120**, 087401 (2018).
- [31] B. Höckendorf, A. Alvermann, and H. Fehske, Topological origin of quantized transport in non-Hermitian Floquet chains, *Phys. Rev. Res.* **2**, 023235 (2020).
- [32] A. Banerjee and A. Narayan, Controlling exceptional points with light, *Phys. Rev. B* **102**, 205423 (2020).
- [33] T. Banerjee and K. Sengupta, Emergent conservation in the Floquet dynamics of integrable non-Hermitian models, *Phys. Rev. B* **107**, 155117 (2023).
- [34] S. Ke, W. Wen, D. Zhao, and Y. Wang, Floquet engineering of the non-Hermitian skin effect in photonic waveguide arrays, *Phys. Rev. A* **107**, 053508 (2023).
- [35] Y. Li, C. Lu, S. Zhang, and Y.-C. Liu, Loss-induced Floquet non-Hermitian skin effect, *Phys. Rev. B* **108**, L220301 (2023).
- [36] J. Gong and Q.-H. Wang, Stabilizing non-Hermitian systems by periodic driving, *Phys. Rev. A* **91**, 042135 (2015).
- [37] A. McDonald and A. A. Clerk, Exponentially-enhanced quantum sensing with non-Hermitian lattice dynamics, *Nat. Commun.* **11**, 5382 (2020).
- [38] M. De Carlo, F. De Leonardis, S. R.A., L. Colatorti, and V. Passaro, Non-Hermitian sensing in photonics and electronics: A review., *Sensors* **22**, 3977 (2022).
- [39] S. Weidemann, M. Kremer, T. Helbig, T. Hofmann, A. Stegmaier, M. Greiter, R. Thomale, and A. Szameit, Topological funneling of light, *Science* **368**, 311 (2020).
- [40] H. Jiang, L.-J. Lang, C. Yang, S.-L. Zhu, and S. Chen, Interplay of non-Hermitian skin effects and Anderson localization in nonreciprocal quasiperiodic lattices, *Phys. Rev. B* **100**, 054301 (2019).
- [41] S. Aubry and G. André, Analyticity breaking and Anderson localization in incommensurate lattices, *Ann. Isr. Phys. Soc.* **3**, 133 (1980).
- [42] P. G. Harper, Single band motion of conduction electrons in a uniform magnetic field, *Proc. Phys. Soc. Sect. A* **68**, 874 (1955).
- [43] D. C. Brody, Biorthogonal quantum mechanics, *J. Phys. A: Math. Theor.* **47**, 035305 (2014).
- [44] Since the Floquet propagator turns out to be nonunitary, we can explicitly keep the unitarity conserved at each time step using the QR decomposition, as demonstrated in recent works. We have checked that any qualitative result in this work remains unaffected after preservation of the unitarity.
- [45] F. Evers and A. D. Mirlin, Fluctuations of the inverse participation ratio at the anderson transition, *Phys. Rev. Lett.* **84**, 3690 (2000).
- [46] S. Wessel and I. Milat, Quantum fluctuations and excitations in antiferromagnetic quasicrystals, *Phys. Rev. B* **71**, 104427 (2005).
- [47] P. Wang, L. Jin, and Z. Song, Non-Hermitian phase transition and eigenstate localization induced by asymmetric coupling, *Phys. Rev. A* **99**, 062112 (2019).
- [48] S. Rahav, I. Gilary, and S. Fishman, Effective Hamiltonians for periodically driven systems, *Phys. Rev. A* **68**, 013820 (2003).
- [49] N. Goldman and J. Dalibard, Periodically driven quantum systems: Effective Hamiltonians and engineered gauge fields, *Phys. Rev. X* **4**, 031027 (2014).
- [50] L. D. Marin Bukov and A. Polkovnikov, Universal high-frequency behavior of periodically driven systems: From dynamical stabilization to Floquet engineering, *Adv. Phys.* **64**, 139 (2015).
- [51] A. Eckardt and E. Anisimovas, High-frequency approximation for periodically driven quantum systems from a Floquet-space perspective, *New J. Phys.* **17**, 093039 (2015).
- [52] S. Longhi, Stochastic non-Hermitian skin effect, *Opt. Lett.* **45**, 5250 (2020).
- [53] D. N. Makarov, Theory of a frequency-dependent beam splitter in the form of coupled waveguides, *Sci. Rep.* **11**, 5014 (2021).